

# OPTIMUM ABSORBER PARAMETERS FOR TUNED LIQUID COLUMN DAMPERS

By Swaroop K. Yalla,<sup>1</sup> Student Member, ASCE, and Ahsan Kareem,<sup>2</sup> Member, ASCE

**ABSTRACT:** Tuned liquid column dampers (TLCDs) are a class of tuned liquid dampers that impart indirect damping to the primary structure through oscillations of the liquid column in a U-shaped container. The energy dissipation in the water column results from the passage of the liquid through an orifice with inherent head-loss characteristics. The overall damping in a TLCD depends on the head-loss coefficient and the velocity of the oscillating liquid, and it is nonlinear due to the quadratic damping term. Using the TLCD theory and the equivalent linearization scheme, a new approach has been developed that helps to compute the optimum head-loss coefficient for a given level of wind or seismic excitation in a single step, without resorting to iterations. The optimal damping coefficient and tuning ratio of a TLCD using a single degree of freedom system under the white noise and a set of filtered white noise excitations representing wind and seismic loadings is presented. Optimum values of damping have also been investigated for multiple TLCDs. An example is presented to demonstrate the performance of multiple TLCDs in controlling multiple modes under wind excitation.

## INTRODUCTION

The increasing height and span of structures is resulting in their increased vulnerability to environmental forces such as winds and earthquakes. In addition to structural failure possibilities, issues such as functional performance and human discomfort are major concerns. To improve the design and performance of these structures, several design modifications are available. One of the most promising alternatives is to add external damping devices to the structures. Research on devices of this type has been extensive, and many buildings have already been equipped with such control devices (Soong and Dargush 1997; Kijewski et al. 1998). Tuned liquid column dampers (TLCDs) are a class of tuned liquid dampers that impart external damping to a structure through an oscillating liquid column in a U-shaped container (Sakai and Takaeda 1989; Xu et al. 1992; Kareem 1993). Energy dissipation in the water column is due to the passage of the liquid through an orifice with inherent head-loss characteristics (Fig. 1).

In the classical work on the dynamic vibration absorber, Den Hartog (1956) derived expressions for the optimum damping ratio and tuning ratio (i.e., ratio of the absorber frequency to the natural frequency of the primary system) for an undamped mass subjected to harmonic excitation. The optimum absorber parameters that minimize the displacement response of the primary system were found to be simple functions of the mass ratio. McNamara (1977) reported design of tuned mass dampers (TMDs) for buildings with attention to experimental designs and design considerations. Ioi and Ikeda (1978) developed empirical expressions to determine correction factors for optimum parameters in the case of lightly damped structures. Randall et al. (1981) and Warburton and Ayorinde (1980) further tabulated and developed design charts for the optimum parameters for specified mass ratios and different primary system damping. Warburton (1982) presented optimal parameters for TMDs under random excitations idealized by white noise. In this paper, similar expressions have been developed and parameters have been tabulated for un-

damped and damped primary systems equipped with TLCDs. In the design of TMDs for wind and earthquake excitations, the optimum parameters are typically chosen to be those given for a white noise random excitation. In this study, in addition to the white noise excitation, a set of filtered white noise (FWN) excitations has been considered for evaluating the optimal absorber parameters.

Previous work has been done with the aim of deriving optimum parameters for TLCDs. Abé et al. (1996) derived optimum parameters using perturbation techniques. Gao et al. (1997) studied numerically the optimization of TLCDs for sinusoidal excitations. This paper uses a closed-form solution for the integral involved in the estimation of the mean square response and derives the optimal parameters that minimize the variance of the displacement of the primary system. Finally, optimum values of damping also have been investigated for the case of multiple TLCDs. An example has been presented on the efficacy of multiple TLCDs in controlling multiple structural modes under wind excitation.

## ANALYTICAL MODEL

For the coupled structure-TLCD system, the equations of motion are given by

$$\begin{bmatrix} M_s + m_d & \alpha m_d \\ \alpha m_d & m_d \end{bmatrix} \begin{bmatrix} \ddot{X}_s \\ \ddot{X}_f \end{bmatrix} + \begin{bmatrix} C_s & 0 \\ 0 & c_{eq} \end{bmatrix} \begin{bmatrix} \dot{X}_s \\ \dot{X}_f \end{bmatrix} + \begin{bmatrix} K_s & 0 \\ 0 & k_f \end{bmatrix} \begin{bmatrix} X_s \\ X_f \end{bmatrix} = \begin{bmatrix} F \\ \Delta m_d F \\ M_s \end{bmatrix}, \quad |X_f| \leq \frac{(l-b)}{2} \quad (1)$$

where  $X_s$  = response of the primary system;  $X_f$  = response of

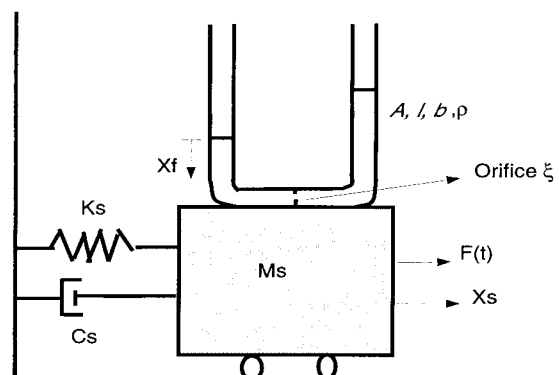


FIG. 1. Schematic Diagram of TLCD Mounted on SDOF System

<sup>1</sup>Grad. Res. Asst., NatHaz Modeling Lab., Dept. of Civ. Engrg. and Geological Sci., Univ. of Notre Dame, Notre Dame, IN 46556.

<sup>2</sup>Robert M. Moran, Prof. and Chair, Dept. of Civ. Engrg. and Geological Sci., Univ. of Notre Dame, Notre Dame, IN.

Note. Associate Editor: Timothy A. Reinhold. Discussion open until January 1, 2001. To extend the closing date one month, a written request must be filed with the ASCE Manager of Journals. The manuscript for this paper was submitted for review and possible publication on February 17, 1999. This paper is part of the *Journal of Structural Engineering*, Vol. 126, No. 8, August, 2000. ©ASCE, ISSN 0733-9445/00/0008-0906-0915/\$8.00 + \$.50 per page. Paper No. 20300.

the liquid damper;  $M_s$  = mass of the primary system;  $K_s$  = stiffness of the primary system;  $C_s$  = damping of the primary system,  $2M_s\zeta_s\omega_s$ ;  $c_{eq}$  = equivalent damping of the liquid damper,  $2m_d\omega_d\zeta$ ;  $\zeta_s$  = damping ratio of the primary system;  $\zeta$  = damping ratio of TLCD;  $\omega_d$  = natural frequency of the liquid damper;  $\omega_s$  = natural frequency of the primary system;  $k_f$  = stiffness of the liquid column,  $2\rho Ag$ ;  $m_d$  = mass of liquid in the tube,  $\rho Al$ ;  $\rho$  = liquid density;  $A$  = cross-sectional area of the tube;  $\alpha$  = length ratio,  $b/l$ ;  $l$  = length of the liquid column;  $b$  = horizontal length of the column;  $g$  = gravitational constant;  $F(t)$  = force acting on the primary system; and  $\Delta = 1$  for base excitation where  $X_s$  = relative displacement; and  $\Delta = 0$  for primary system excitation where  $X_s$  = absolute displacement.

The actual nonlinearity due to quadratic damping in the equation of motion of TLCD is given

$$c_{nonlinear} = \frac{1}{2} \rho A \xi |\dot{X}_f(t)|$$

An equivalent linearized damping coefficient  $c_{eq}$  has been used to replace the nonlinear damping term. The equivalent linearization technique and its implications on  $\xi$ , the head-loss coefficient, is addressed in the fourth section. Introducing the following nondimensional quantities:

Mass ratio:

$$\mu = \frac{m_d}{M_s}$$

Tuning ratio:

$$\gamma = \frac{\omega_d}{\omega_s}$$

and defining the transfer functions in the frequency domain

$$H(i\omega) = \frac{X_s(i\omega)}{F(i\omega)}$$

$$G(i\omega) = \frac{X_f(i\omega)}{F(i\omega)}$$

the following expressions are obtained

$$H(i\omega) = [-\Delta\mu\alpha(i\omega)^2 + (i\omega)^2 + 2\zeta\omega_d(i\omega) + \omega_d^2]$$

$$/ \{ [(i\omega)^2(1 + \mu) + 2\zeta_s\omega_s(i\omega) + \omega_s^2] \}$$

$$\cdot [(i\omega)^2 + 2\zeta\omega_d(i\omega) + \omega_d^2] - (i\omega)^4\alpha^2\mu \}$$

$$G(i\omega) = [-\alpha(i\omega)^2 + \Delta] / \{ [(i\omega)^2(1 + \mu) + 2\zeta_s\omega_s(i\omega) + \omega_s^2]$$

$$\cdot [(i\omega)^2 + 2\zeta\omega_d(i\omega) + \omega_d^2] - (i\omega)^4\alpha^2\mu \}$$

One can compute the response quantities of interest using random vibration analysis. In particular, the quantities of interest are the variance of the primary system displacement and the variance of the liquid velocity in the TLCD. The latter quantity will be used in the fourth section to compute the optimum head-loss coefficient for the orifice. The response quantities are obtained

$$\sigma_{x_s}^2 = \int_{-\infty}^{\infty} |H(\omega)|^2 S_f(\omega) d\omega \quad (2)$$

$$\sigma_{\dot{x}_f}^2 = \int_{-\infty}^{\infty} \omega^2 |G(\omega)|^2 S_f(\omega) d\omega \quad (3)$$

where  $S_f(\omega)$  = power spectral density of the forcing function. A simplified solution to the integral for random vibration analysis has been used to evaluate (2) and (3) (Roberts and Spanos

TABLE 1. Example Forcing Functions

Type of excitation (1)	$S_f(\omega)$ spectrum (2)
White noise (primary system)	$S_0$
FOF (primary system)	$\frac{S_0}{v^2 + \omega^2}$
SOF (primary system and/or base)	$\frac{S_0\{c^2\omega^2 + d^2\}}{[b^2 - \omega^2]^2 + a^2\omega^2}$

1990). Three representative forcing functions have been studied here, as listed in Table 1.

Based on these three excitation models, optimal damping ratios have been obtained for both the damped and undamped primary systems. It has been noted that one can derive an explicit expression for an undamped mass subjected to white noise. However, for damped systems and/or other excitations, the development of closed-form solutions is challenging. This is because some characteristics of the classical damper system, like invariance points, do not exist when damping is introduced in the primary system (Den Hartog 1956). Therefore, the optimal absorber parameters must be obtained numerically for these cases. The optimal conditions are given by

$$\frac{\partial \sigma_{x_s}^2}{\partial \zeta} = 0; \quad \frac{\partial \sigma_{x_s}^2}{\partial \gamma} = 0 \quad (4)$$

Solving the conditions in (4) symbolically, using X-Maple software,  $\zeta_{opt}$  and  $\gamma_{opt}$  can be obtained.

## OPTIMUM ABSORBER PARAMETERS

In this section, optimal parameters are derived for the forcing functions listed in Table 1.

### White Noise Excitation

The response integral in (2) and (3) can be cast in the following form:

$$\sigma_{x_s}^2 = S_0 \int_{-\infty}^{\infty} \frac{\Xi_n(\omega) d\omega}{\Lambda_n(-i\omega)\Lambda_n(i\omega)} \quad (5)$$

where  $n$  = order of the scheme that varies for the three cases. For a primary system excited by white noise,  $n = 4$ . The integrals are evaluated using the expressions given in Roberts and Spanos (1990)

$$\sigma_{x_s}^2 = \frac{\begin{bmatrix} 0 & \chi_2 & \chi_1 & \chi_0 \\ -\lambda_4 & \lambda_2 & -\lambda_0 & 0 \\ 0 & -\lambda_3 & \lambda_1 & 0 \\ 0 & \lambda_4 & -\lambda_2 & \lambda_0 \end{bmatrix} \pi S_0}{\lambda_4} ; \quad \sigma_{\dot{x}_f}^2 = \frac{\begin{bmatrix} \chi_3 & 0 & 0 & 0 \\ -\lambda_4 & \lambda_2 & -\lambda_0 & 0 \\ 0 & -\lambda_3 & \lambda_1 & 0 \\ 0 & \lambda_4 & -\lambda_2 & \lambda_0 \end{bmatrix} \pi S_0}{\lambda_4} \quad (6)$$

in which

$$\chi_0 = \omega_d^4; \quad \chi_1 = 4\zeta^2\omega_d^2 - 2\omega_d^2; \quad \chi_2 = 1; \quad \chi_3 = \alpha^2; \quad \lambda_0 = \omega_d^2\omega_s^2;$$

$$\lambda_1 = 2\omega_d^2\zeta_s\omega_s + 2\zeta\omega_d\omega_s^2; \quad \lambda_2 = \omega_d^2(1 + \mu) + 4\zeta\omega_d\omega_s\zeta_s + \omega_s^2;$$

$$\lambda_3 = 2\zeta\omega_d(1 + \mu) + 2\zeta_s\omega_s; \quad \lambda_4 = 1 + \mu - \alpha^2\mu$$

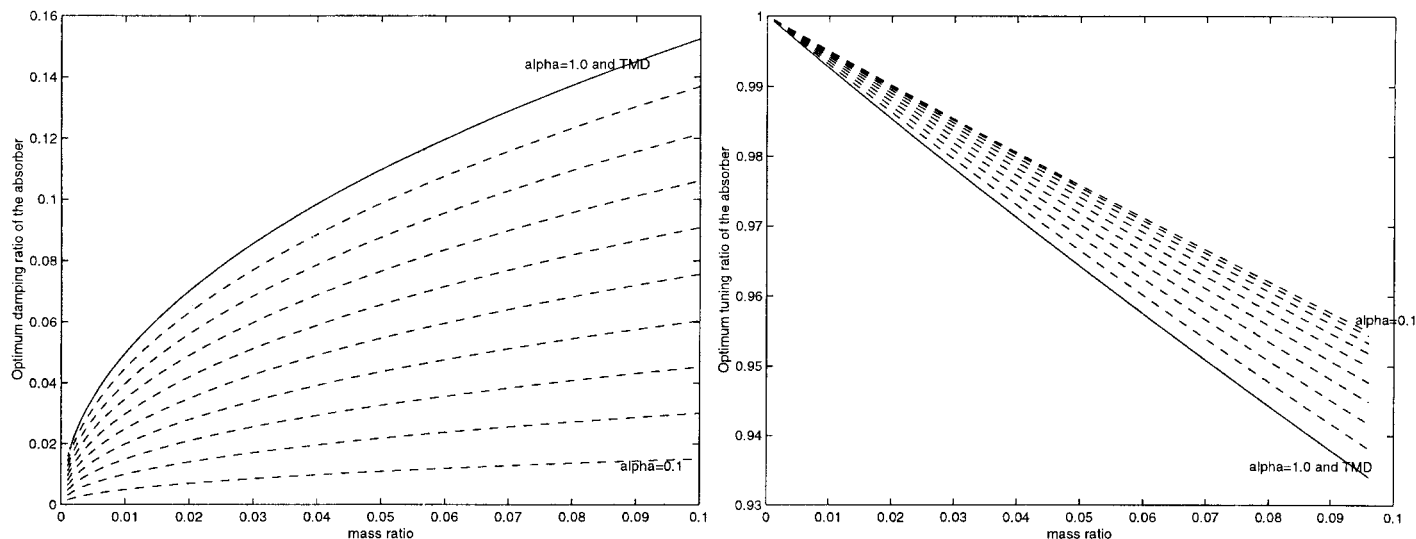


FIG. 2. Comparison of Optimum Absorber Parameters for TLCD with Varying  $\alpha$  and for TMD

### Undamped Primary System

Solving the two optimization conditions in (4) and setting  $\zeta_s = 0$ , multiple sets of optimum values are obtained. However, only one set contains both positive values, which are given

$$\zeta_{opt} = \frac{\alpha}{2} \sqrt{\frac{2\mu \left( \alpha^2 \frac{\mu}{4} - \mu - 1 \right)}{(\alpha^2 \mu^2 + \alpha^2 \mu - 4\mu - 2\mu^2 - 2)}} \quad (7a)$$

$$\gamma_{opt} = \frac{\sqrt{1 + \mu \left( 1 - \frac{\alpha^2}{2} \right)}}{1 + \mu} \quad (7b)$$

In an earlier work (Yalla et al. 1998), the authors showed that keeping the tuning ratio equal to 1 results in a similar expression for the optimal damping given by

$$\zeta_{opt} = \frac{1}{2} \sqrt{\frac{\mu(\mu + \alpha^2)}{1 + \mu}} \quad (8)$$

This is justifiable because for the low mass ratios of the order 1–5% utilized mainly for tall buildings the tuning ratio is close to 1, and in this case the optimal damping coefficient given by (8) approximates (7) quite well. Similar expressions exist for an optimal damping coefficient and tuning ratio of a TMD given by Warburton and Ayorinde (1980)

$$\zeta_{opt} = \frac{1}{2} \sqrt{\frac{\mu(1 + 0.75\mu)}{(1 + \mu)(1 + 0.5\mu)}} \quad (9a)$$

$$\gamma_{opt} = \frac{\sqrt{1 + 0.5\mu}}{1 + \mu} \quad (9b)$$

In all cases considered, the optimum damping coefficient is independent of the value of  $S_0$ , the intensity of white noise excitation. Therefore, it has been kept equal to unity in this study. It is noteworthy that (7) reduces to (9) as  $\alpha$  approaches 1.

Fig. 2 shows how (7) and (9) vary with the mass ratio. As the length ratio increases, the damping ratio increases, because there is more mass in the horizontal portion of the TLCD. This contributes to indirect damping, which means it is better to keep the length ratio as high as possible without violating the constraints of (1) or the limitations of other structural or architectural considerations. Moreover, note that at  $\alpha = 1$  (i.e., when only the horizontal portion of the liquid is acting), it is

effectively behaving like an equivalent TMD. However, in this case the secondary system no longer retains the U-shape and therefore ceases to function as a TLCD.

### Damped Primary System

As discussed earlier, it is not convenient to obtain a closed-form solution for optimum damper parameters for a damped primary system; therefore, it must be estimated numerically (Warburton 1982). These computations have been conducted for  $\zeta_s = 1, 2$ , and 5% and  $\mu = 0.5, 1, 1.5, 2$ , and 5%, and optimum absorber parameters are presented in Table 2 along with the undamped case.

Table 2 shows that as the mass ratio increases,  $\zeta_{opt}$  also increases. Eq. (7) verifies this for the undamped case, because it is approximately proportional to the square root of the mass ratio. The tuning ratio also decreases as the mass ratio and the damping in the primary system increase, which is consistent with the results obtained for tuned mass dampers. It is observed that for small values of  $\zeta_s$ ,  $\zeta_{opt}$  is not affected; therefore for a lightly damped system, the optimum absorber parameters derived for an undamped primary system are valid. For higher levels of damping in the primary system, one can derive empirical expressions for the optimum damping ratio as a function of the primary system damping ratio.

### First-Order Filter (FOF)

The forcing function now has a spectrum given by

$$S_f(\omega) = \frac{S_0}{\nu^2 + \omega^2} \quad (10)$$

This type of function can be used to approximate wind-in-

TABLE 2. Optimum Absorber Parameters for White Noise Excitation for Various Mass Ratios

$\mu$ (%)	Undamped Primary System		1% Damping		2% Damping		5% Damping	
	$\gamma_{opt}$ (2)	$\zeta_{opt}$ (3)	$\gamma_{opt}$ (4)	$\zeta_{opt}$ (5)	$\gamma_{opt}$ (6)	$\zeta_{opt}$ (7)	$\gamma_{opt}$ (8)	$\zeta_{opt}$ (9)
0.5	0.9965	0.0317	0.9962	0.0317	0.9958	0.0317	0.995	0.0317
1	0.993	0.0448	0.9925	0.0448	0.9921	0.0448	0.9908	0.0448
1.5	0.9896	0.0547	0.989	0.0547	0.9885	0.0547	0.9869	0.0547
2	0.986	0.0631	0.9855	0.0631	0.985	0.0631	0.983	0.0631
5	0.966	0.0986	0.965	0.0986	0.964	0.0986	0.962	0.0986

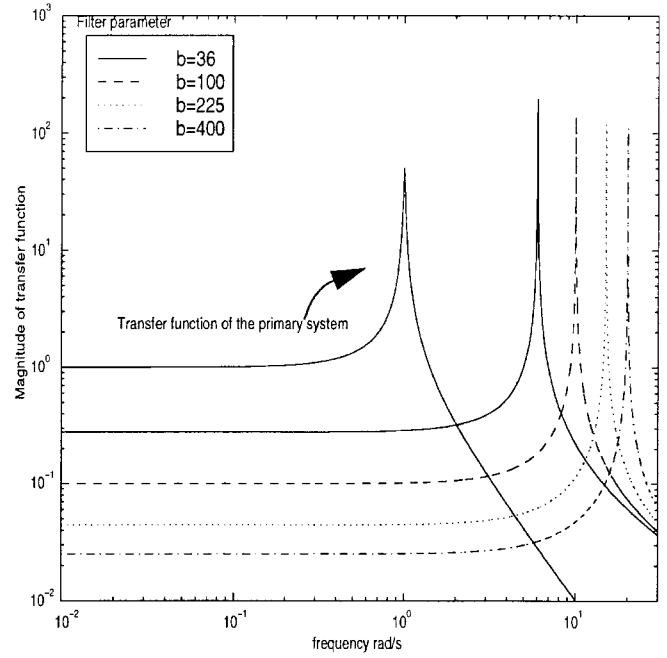
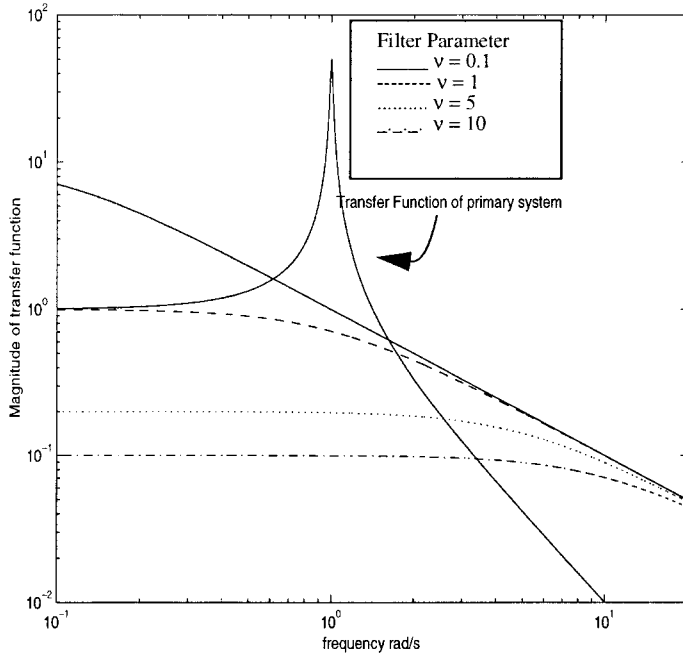


FIG. 3. Transfer Function of Filters and Primary System: (a) FOFs; (b) SOFs

duced positive pressures for the along-wind loading. In this case, the order of integration in the denominator increases to 5 and the rest of the procedure remains the same. Following the similar method used previously, integrals for estimating variances of the displacement of the primary system and the liquid velocity provide

$$\sigma_{x_i}^2 = \frac{\begin{bmatrix} 0 & 0 & \chi_2 & \chi_1 & \chi_0 \\ -\lambda_5 & \lambda_3 & -\lambda_1 & 0 & 0 \\ 0 & -\lambda_4 & \lambda_2 & -\lambda_0 & 0 \\ 0 & \lambda_5 & -\lambda_3 & \lambda_1 & 0 \\ 0 & 0 & \lambda_4 & -\lambda_2 & \lambda_0 \end{bmatrix} \pi S_0}{\lambda_5}; \quad \sigma_{\dot{x}_j}^2 = \frac{\begin{bmatrix} 0 & \chi_3 & 0 & 0 & 0 \\ -\lambda_5 & \lambda_3 & -\lambda_1 & 0 & 0 \\ 0 & -\lambda_4 & \lambda_2 & -\lambda_0 & 0 \\ 0 & \lambda_5 & -\lambda_3 & \lambda_1 & 0 \\ 0 & 0 & \lambda_4 & -\lambda_2 & \lambda_0 \end{bmatrix} \pi S_0}{\lambda_5} \quad (11)$$

in which

$$\begin{aligned} \lambda_5 &= 1 + \mu - \alpha^2; \quad \lambda_4 = \nu(1 + \mu - \alpha^2) + 2\zeta_s \omega_s + 2\zeta \omega_d(1 + \mu); \\ \lambda_3 &= \nu(2\zeta \omega_d(1 + \mu) + 2\zeta_s \omega_s) + \omega_d^2(1 + \mu) + 4\zeta \omega_d \zeta_s \omega_s + \omega_s^2; \\ \lambda_2 &= \nu(\omega_d^2(1 + \mu) + 4\zeta \omega_d \zeta_s \omega_s + \omega_s^2) + 2\zeta \omega_d \omega_s^2 + 2\omega_d^2 \zeta_s \omega_s; \\ \lambda_1 &= \nu(2\zeta \omega_d \omega_s^2 + 2\omega_d^2 \zeta_s \omega_s) + \omega_d^2 \omega_s^2; \quad \lambda_0 = \nu \omega_d^2 \omega_s^2 \end{aligned}$$

Fig. 3(a) shows the transfer functions of the FOF with different values of the parameter  $\nu$  and the transfer function of the primary system. Also shown for reference is the transfer function of the primary system. Table 3 gives the optimum absorber parameters for these FOFs. Note that when  $\nu = 10$ , the optimum parameters are the same as those obtained for white noise, because the filter is fairly uniform, like white noise excitation, around the natural frequency of the primary system. However, for other cases (e.g.,  $\nu = 0.1$  and 1), the optimum parameters are slightly different. The effect is more pronounced in the case of the tuning ratio and increases as the damping in the primary system increases. Optimum parameters

TABLE 3. Optimum Absorber Parameters for FOF for Different Parameter  $\nu$

Parameter of FOF (1)	$\gamma_{opt}$ (2)	$\zeta_{opt}$ (3)
$\nu = 0.1$	0.991	0.04477
$\nu = 1$	0.992	0.04476
$\nu = 5$	0.9925	0.04483
$\nu = 10$	0.993	0.04482

Note: These values are computed for undamped primary system with  $\mu = 1\%$ .

TABLE 4. Optimum Absorber Parameters for FOF for Various Mass Ratios

$\nu = 1$ (1)	Undamped Primary System		1% Damping		2% Damping		5% Damping	
	$\gamma_{opt}$ (2)	$\zeta_{opt}$ (3)	$\gamma_{opt}$ (4)	$\zeta_{opt}$ (5)	$\gamma_{opt}$ (6)	$\zeta_{opt}$ (7)	$\gamma_{opt}$ (8)	$\zeta_{opt}$ (9)
$\mu = 0.5\%$	0.993	0.0320	0.992	0.0319	0.991	0.0318	0.988	0.0317
$\mu = 1\%$	0.992	0.0448	0.991	0.0447	0.990	0.0447	0.987	0.0445
$\mu = 1.5\%$	0.986	0.0548	0.985	0.0547	0.984	0.0547	0.979	0.0545
$\mu = 2\%$	0.984	0.0630	0.983	0.0629	0.981	0.0629	0.9878	0.0626
$\mu = 5\%$	0.962	0.0980	0.960	0.0979	0.958	0.0978	0.953	0.0973

have been computed for  $\nu = 1$  and tabulated in Table 4. Though the optimal parameters can be obtained through the simultaneous solution of the two nonlinear equations resulting from (4) the task becomes computationally intensive for the FOFs and second-order filters (SOFs). In this study, optimal parameters were obtained by utilizing the MATLAB optimization toolbox (Grace 1992).

## SOF

A general SOF studied here has the following spectral description:

$$S_f(\omega) = \frac{S_0\{c^2\omega^2 + d^2\}}{\{[b^2 - \omega^2]^2 + a^2\omega^2\}} \quad (12)$$

where  $a$ ,  $b$ ,  $c$ , and  $d$  = parameters of the filter. The SOFs can be used to represent earthquake and wind excitations. For earthquakes, the excitation is through the base, whereas in the case of wind, the wind pressure acts directly on the primary system. The expression in (12) describes the well-known Kanai-Tajimi spectrum, given as [e.g., Clough and Penzien (1993)]

$$S_f(\omega) = \frac{S_0 \left[ 1 + 4\zeta_g^2 \left( \frac{\omega}{\omega_g} \right)^2 \right]}{\left\{ \left[ 1 - \left( \frac{\omega}{\omega_g} \right)^2 \right]^2 + 4\zeta_g^2 \left( \frac{\omega}{\omega_g} \right)^2 \right\}} \quad (13)$$

where  $\omega_g$  = dominant ground frequency; and  $\zeta_g$  = ground damping factor.

Similarly, the across-wind excitation can be modeled as a FWN using a SOF. Kareem (1983, 1984) has proposed the following empirical expression for the spectral density of the across-wind force for square buildings:

$$\frac{nS_f(z, n)}{\sigma_f^2} = \alpha_0 \beta_0 \left( \frac{n}{n_s} \right)^\delta \quad (14)$$

where

$$\alpha_0 = \frac{b}{\left[ 1 - \left( \frac{n}{n_s} \right)^2 \right]^2 + \left[ 2b \left( \frac{n}{n_s} \right) \right]^2}$$

$$\beta_0 = 1.32 \left[ \left( \frac{1}{3\tilde{\alpha}} \right)^{0.5} + 0.154 \left( 1 - \frac{z}{H} \right)^{3.5} \right]$$

where  $n_s$  = shedding frequency;  $S\bar{U}(z)/B$ ;  $B$  = breadth of the building;  $\bar{U}(z)$  = mean speed at height  $z$ ;  $S$  = Strouhal number;  $\sigma_f^2$  = mean square value of the fluctuating across-wind force;  $\tilde{\alpha}$  = exponent term in the power law of the wind velocity profile;  $H$  = height of the building;  $b$  = bandwidth coefficient,  $\sqrt{2}I(z)$ ;  $I(z)$  = turbulence intensity at height  $z$ ; and  $\delta = 0.9$  for  $n \leq n_s$  and  $3.0$  for  $n > n_s$ . The across-wind loading model can be represented by (12).

The magnitude of the transfer function of the filter given by (12) is shown in Fig. 3(b) for parameters  $a = 0.01$ ,  $c = 1$ ,  $d = 10$ , and varying  $b = 36, 100, 225$ , and  $400$ . Table 5 shows how the optimal parameters are influenced as the filter parameter  $b$  changes. As  $b$  increases, the assumption of purely white noise becomes valid and the solution approaches that for the white noise case. The other parameters have been kept the same and optimal parameters have been computed for damped and undamped cases (Table 6). The details of the integration scheme are given in Yalla and Kareem (1998).

As in previous cases,  $\zeta_{opt}$  decreases as the damping in the primary system increases and increases as the mass ratio increases; however, the damping in the primary system affects  $\zeta_{opt}$  more in this case than in the case of white noise. In addition, the tuning ratio slightly departs from  $\gamma = 1.00$  as the damping in the primary system increases.

**TABLE 5. Optimum Absorber Parameters for SOF for Different Values of  $b$**

Parameter of SOF (1)	$\gamma_{opt}$ (2)	$\zeta_{opt}$ (3)
$b = 36$	1.05	0.1111
$b = 100$	1.01	0.0702
$b = 225$	1.00	0.0572
$b = 400$	0.995	0.0524

Note: All other parameters are kept constant  $a = 0.01$ ,  $c = 1$ ,  $d = 10$ ,  $\mu = 0.02$ , and  $\zeta_s = 0.05$ .

**TABLE 6. Optimum Absorber Parameters for SOF for Various Mass Ratios**

$\mu^a$ (%)	Undamped Primary System		1% Damping		2% Damping		5% Damping	
	$\gamma_{opt}$ (1)	$\zeta_{opt}$ (2)	$\gamma_{opt}$ (4)	$\zeta_{opt}$ (5)	$\gamma_{opt}$ (6)	$\zeta_{opt}$ (7)	$\gamma_{opt}$ (8)	$\zeta_{opt}$ (9)
0.5	1.04	0.1510	1.04	0.1401	1.045	0.1299	1.05	0.0956
5	1.04	0.1559	1.04	0.1450	1.045	0.1350	1.05	0.1008
1.5	1.04	0.1606	1.04	0.1498	1.045	0.1399	1.05	0.106
2	1.04	0.1654	1.04	0.1546	1.045	0.1448	1.05	0.1111
5	1.04	0.1927	1.04	0.1821	1.045	0.173	1.05	0.1406

<sup>a</sup> $a = 0.01$ ,  $b = 36$ ,  $c = 1$ , and  $d = 10$ .

## OPTIMUM HEAD-LOSS COEFFICIENT

The procedure for estimating the optimum damping coefficient for TLCDs under a host of loading conditions was outlined in previous sections. In the case of TLCDs, the associated optimal head-loss coefficient needs to be determined. This is the parameter responsible for introducing damping in the liquid column of the TLCD. Using the statistical linearization method, one can write the error between the non-linear and equivalent linear system

$$\varepsilon = \frac{1}{2} \rho A \xi |\dot{X}_f| \dot{X}_f - c_{eq} \dot{X}_f \quad (15)$$

The equivalent damping coefficient can be obtained by minimizing the mean square value of the error, which results in the following expression for the equivalent damping (assuming the liquid velocity to be Gaussian):

$$c_{eq} = \sqrt{\frac{2}{\pi}} \rho A \xi \sigma_{\dot{x}_f} \quad (16)$$

where  $\sigma_{\dot{x}_f}$  = standard deviation of the liquid velocity; and  $\xi$  = head-loss coefficient. Eq. (16) suggests that, because  $\sigma_{\dot{x}_f}$  increases as the loading increases, to maintain the optimal damping  $\xi$  must decrease. Hence there exists an optimal head-loss coefficient at each loading intensity. These variations define the damping characteristics of the orifice needed at different excitation levels. An iterative method has been used in previous studies (Balendra et al. 1995), because the damping term depends on  $\sigma_{\dot{x}_f}$ , which is not known a priori. The second approach, a direct method developed in this study, involves obtaining  $\zeta_{opt}$  as outlined in the previous sections. This value is then substituted into (3) to obtain  $\sigma_{\dot{x}_f}$ . One can then determine  $\xi_{opt}$  using (16). Fig. 4 provides a step-by-step flowchart for the two methods. Fig. 5(a) shows the typical convergence in an iterative method for an undamped single degree of freedom (SDOF) and TLCD system subjected to white noise excitation, where  $\sigma_{x_s}$  and  $\sigma_{\dot{x}_f}$  are calculated by (2) and (3). This is repeated for a range of  $\xi$ , and  $\xi_{opt}$  is determined where the  $\sigma_{x_s}$  is minimum.

This section details explicit expression for one case; an undamped SDOF system subject to white noise with tuning ratio close to unity. The optimum value of the damping coefficient for this case reduces to the expression given in (8). Substituting (8) into (3) and (16) gives

$$\xi_{opt} = \mu \sqrt{\frac{(1 + \mu - \alpha^2 \mu) \left( \frac{\mu + \alpha^2}{1 + \mu} \right)^{3/2}}{S_0}} gl \omega_d \sqrt{\mu} \quad (17)$$

For tuning ratios not equal to unity, one can obtain similar expressions. However, they are cumbersome and can be obtained numerically. Note from (17) that the optimum head-loss coefficient is indirectly proportional to the square root of the

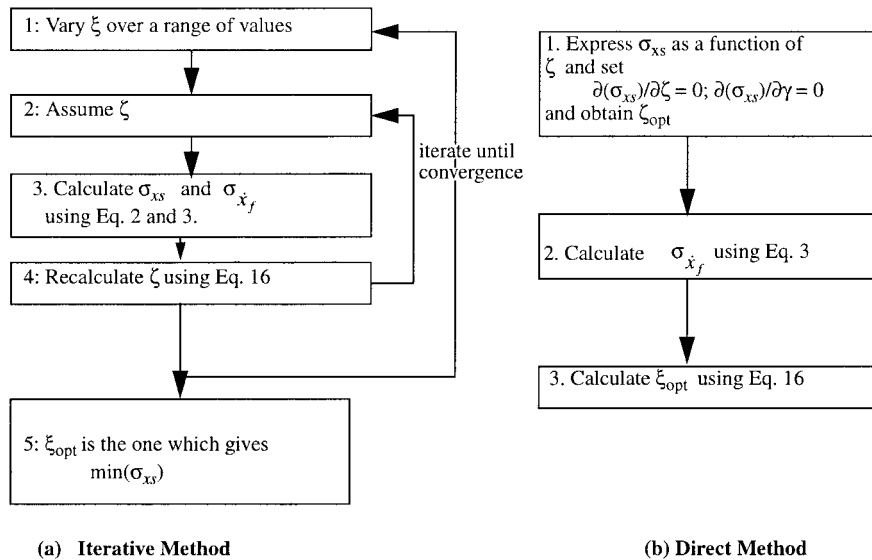


FIG. 4. Flowchart of Two Algorithms

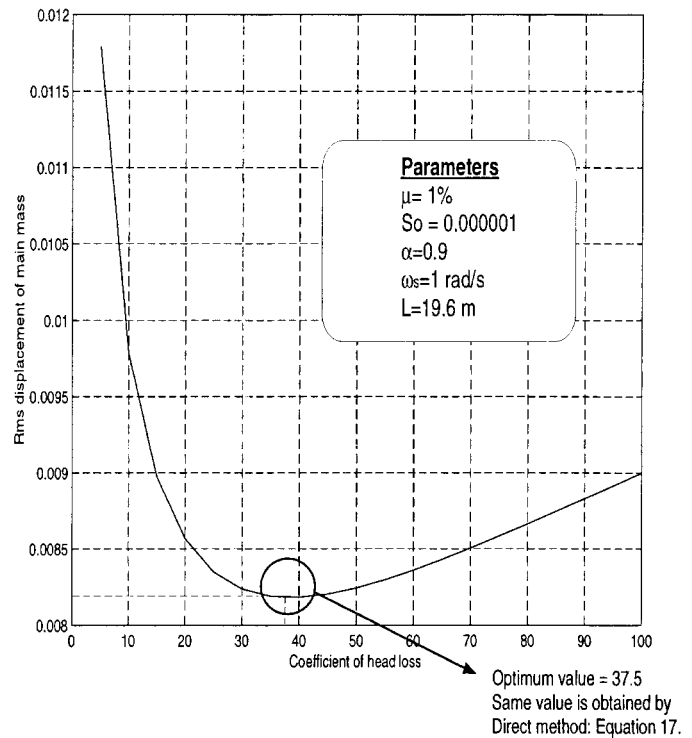
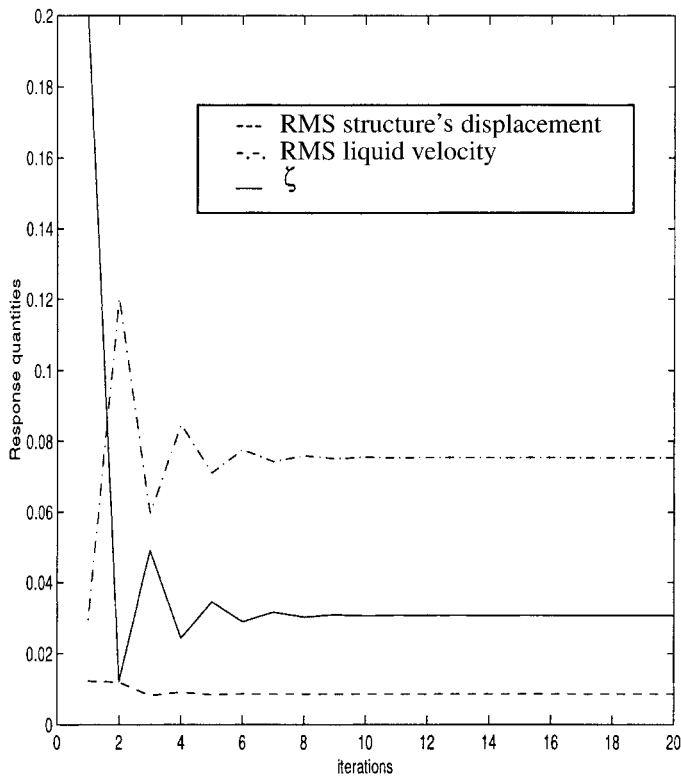


FIG. 5. Iterative Method: (a) Convergence of Response Quantities; (b) Optimum Head-Loss Coefficient

intensity of white noise. Using some representative values, it can be shown that the direct [(17)] and the iterative methods yield the same values [Fig. 5(b)]. However, the direct method is computationally superior, because it does not require iterations, making it more attractive for on-line semiactive control of the orifice.

In Fig. 6 the variation of the optimum head-loss coefficient for various mass ratios under the white noise excitation is shown. Similar trends are noted for the FWN cases (Yalla and Kareem 1998). It is obvious from these curves that at high loading intensities, a very low value of the head-loss coefficient is required. For typical orifice characteristics, this corresponds to 100% orifice opening ratio, i.e., the orifice should be fully open. The relationship between the orifice opening ratio and the head-loss coefficient for standard orifices can be

found in the literature (Blevins 1984) or can be determined experimentally.

## MULTIPLE TLCDs (MTLCDs)

Multiple units of TLCDs can be incorporated in a structural system at one location or distributed spatially. In this system, the multiple secondary systems have their natural frequencies distributed over a range of frequencies. The advantages of such a distributed system is that it is more robust and effective for excitation frequencies distributed over a wide band. In the following study, MTLCD configuration design parameters are evaluated. These are later used to reduce wind-induced response of a structure.

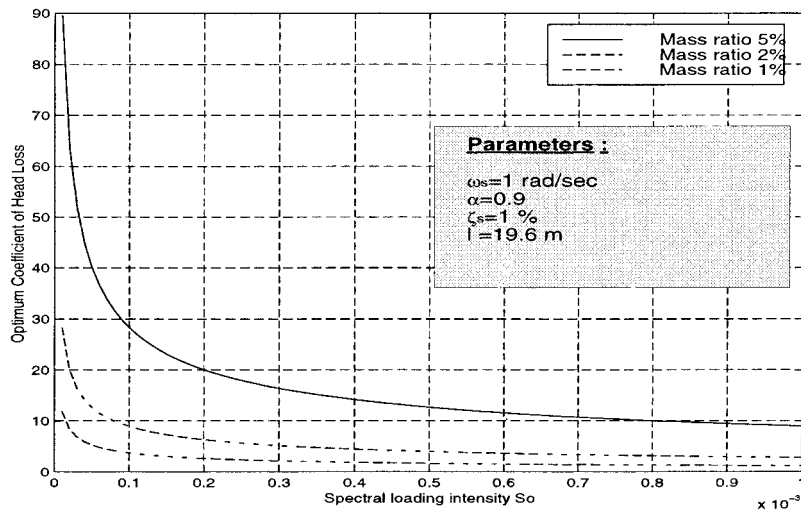


FIG. 6. Variation of Optimum Head-Loss Coefficient with Loading Intensity: White Noise Excitation

### SDOF-MTLCD Configuration

In an SDOF-MTLCD configuration, the primary system is represented by an SDOF system and the secondary system consists of MTLCDs. In the case of a single TMD, Kareem (1983) demonstrated that buildings with well-separated natural frequencies can be adequately represented by an equivalent SDOF primary system. The analysis is simplified when the contribution of the higher modes of the primary system is ignored (Kareem 1981). In this section, the primary system is represented by its first mode. The equations of motion of the SDOF-MTLCD system (Fig. 7) are given

$$\begin{bmatrix} \tilde{m}_s & \underline{m}_d^T \\ \underline{m}_d & \underline{m} \end{bmatrix} \begin{bmatrix} \ddot{X}_s \\ \ddot{X}_{fn} \end{bmatrix} + \begin{bmatrix} C_s & \underline{0} \\ \underline{0} & \underline{c}_{eqn} \end{bmatrix} \begin{bmatrix} \dot{X}_s \\ \dot{X}_{fn} \end{bmatrix} + \begin{bmatrix} K_s & \underline{0} \\ \underline{0} & \underline{k}_{eqn} \end{bmatrix} \begin{bmatrix} X_s \\ X_{fn} \end{bmatrix} = \begin{bmatrix} F \\ \underline{0} \end{bmatrix} \quad (18)$$

where

$$\begin{aligned} \tilde{m}_s &= M_s + \sum_{n=1}^N m_{dn} \\ \underline{m}_d^T &= \alpha[m_{d1}, m_{d2}, \dots, m_{dN}] \\ \underline{m} &= \text{diag}([m_{d1}, m_{d2}, \dots, m_{dN}]) \end{aligned}$$

and  $\underline{c}_{eqn}$  and  $\underline{k}_{eqn} = (n, n)$  diagonal matrices similar to  $\underline{m}$ .

The transfer function of the primary system is obtained by nondimensionalizing (18)

$$H(\omega) = 1 / \left\{ \left[ (i\omega)^2 \left( 1 + \sum_{n=1}^N \mu_{dn} \right) + 2\zeta_s \omega_s (i\omega) + \omega_s^2 \right] - \alpha^2 (i\omega)^4 \sum_{n=1}^N \frac{\mu_{dn}}{[(i\omega)^2 + 2\zeta_n \omega_{dn} (i\omega) + \omega_{dn}^2]} \right\}$$

and the transfer function for each TLCD is given by

$$G_{dn}(\omega) = \frac{-\alpha (i\omega)^2 H(\omega)}{[(i\omega)^2 + 2\zeta_n \omega_{dn} (i\omega) + \omega_{dn}^2]}; \quad n = 1, \dots, N$$

The analysis of MTLCDs is similar to multiple mass dampers, where the important design parameters are the frequency range and damping ratio of the dampers (Kareem and Kline 1995). The frequency range is defined as the total frequency span of the MTLCDs given as  $\Delta f = f_N - f_1$ . The central damper ( $n = (N + 1)/2$ ) is tuned exactly to the natural frequency of the primary system  $f_s$ . It is assumed that  $N$  is an odd number in this analysis. The frequency of each damper is given by

$$\begin{aligned} f_{dn} &= f_s - \frac{\Delta f}{N} n \quad \text{for } 1 \leq n < \frac{N+1}{2} \\ f_{dn} &= f_s \quad \text{for } n = \frac{N+1}{2} \\ f_{dn} &= f_s + \frac{\Delta f}{N} n \quad \text{for } N \geq n > \frac{N+1}{2} \end{aligned}$$

A brief study has been conducted to examine the effects of the number of dampers, frequency range, and damping ratio of the dampers. Optimum values of these parameters have been obtained by selecting parameters that lead to the minimum RMS displacement. A summary of the results is presented below.

#### Effect of Number of Dampers

From Fig. 8(a), one can see the flattening effect of MTLCDs on the transfer function as compared to the classical double peaked function noted in single TLCD (STLCD). The effect of increasing dampers is similar to that of adding damping (i.e., flattening of the frequency response function). However, it also is observed that the frequency response functions of 5, 11, and 21 TLCD groups are very similar. This suggests that a large number of TLCDs do not necessarily mean better performance, thus limiting the advantage of utilizing MTLCDs.

#### Effect of Damping Ratio of Dampers

The damping ratio of MTLCDs is studied for a group of 11 dampers with a fixed frequency range of 0.2 [Fig. 8(b)]. It is

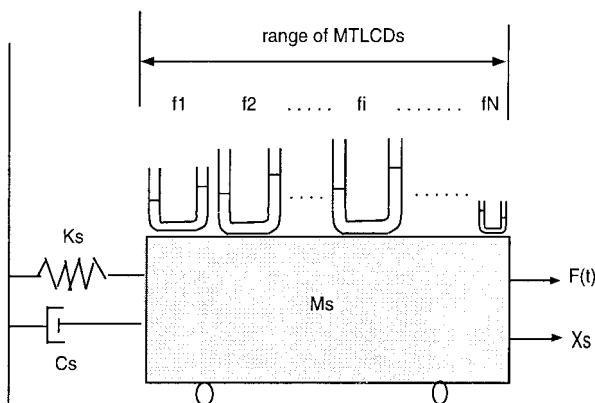


FIG. 7. SDOF-MTLCD Configuration

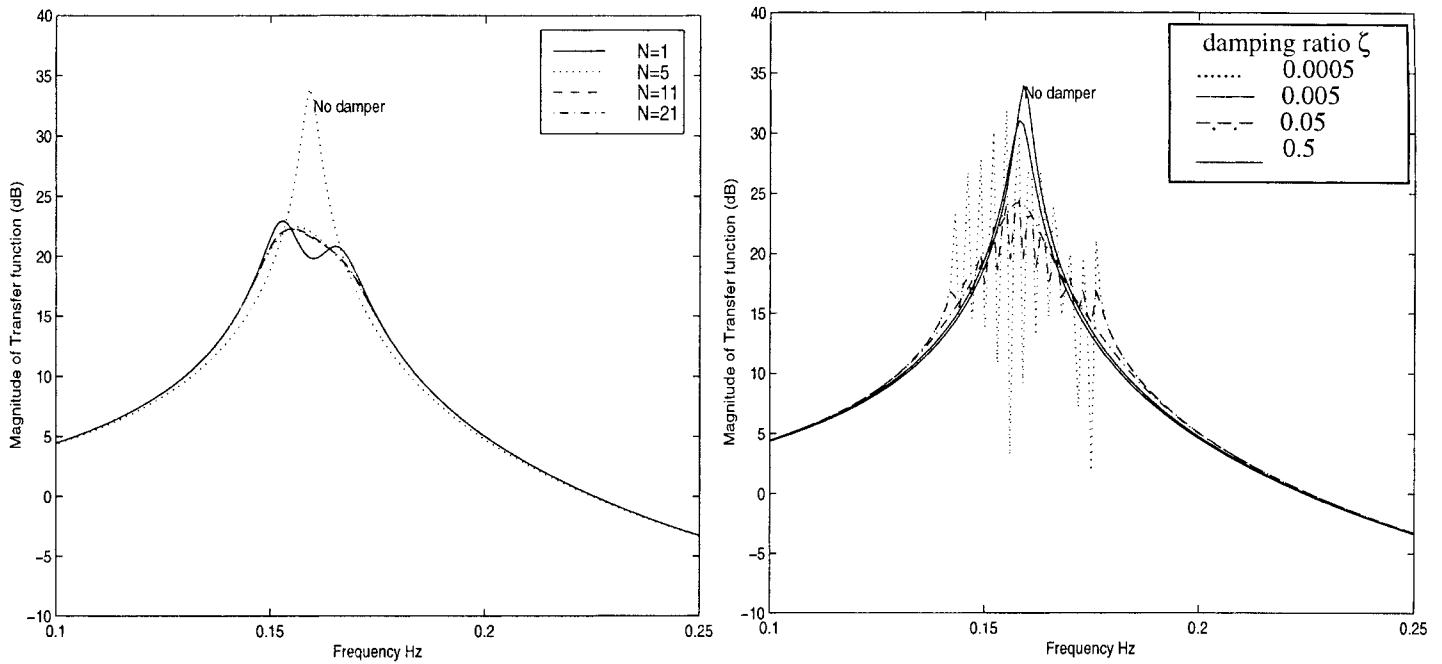


FIG. 8. (a) Effect of Number of Dampers on Frequency Response of SDOF-MTLCD System; (b) Effect of Damping Ratio of Dampers on Frequency Response of SDOF-MTLCD System

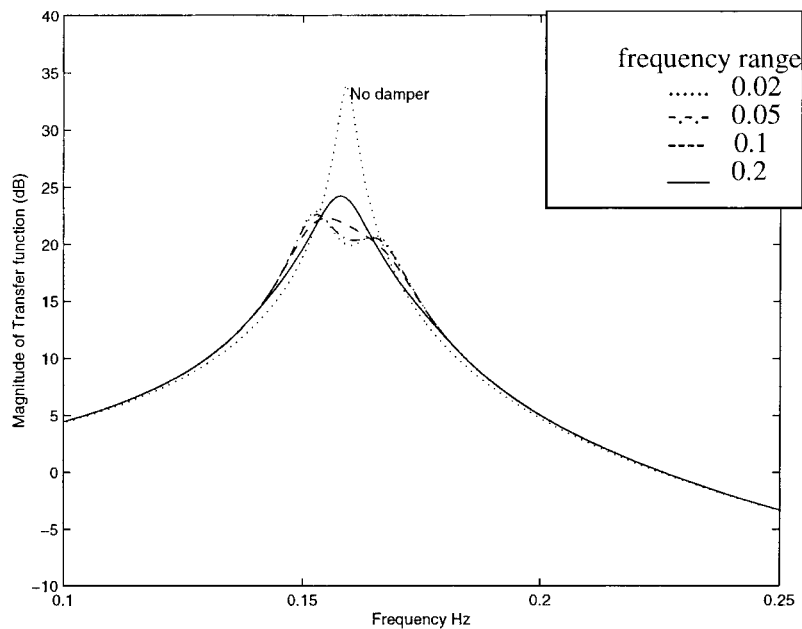


FIG. 9. Effect of Frequency Range on Frequency Response of SDOF-MTLCD System

noted that at low damping ratios, the amplitude of the response function is spiked and has a high transfer function amplitude. As the damping ratio is increased, the response function slowly becomes smoother and the amplitude decreases. After an optimal damping ratio for the dampers is reached, any further increase in the damping ratio results in an increase in the amplitude. This suggests that there exists an optimum damping ratio for a particular set of MTLCD configurations.

#### Effect of Frequency Range

Fig. 9 shows the effect that changing the frequency range has on the frequency response function. It is obvious from the plots that there is an optimum range where the curve flattens

out over a range of frequencies. As the range gets smaller than the optimum, the frequency response for the MTLCD resembles that of an STLCD and so, in a way, the MTLCD loses its effectiveness. The frequency response functions of an STLCD and an MTLCD with a low frequency range (0.02 and smaller) are similar. This is intuitive because there is a practical limit to which one can spread out the MTLCDs over a given frequency range. As this range becomes very small, MTLCDs act almost like an STLCD.

In summary, like in the design of multiple mass dampers, the design of MTLCDs includes two important parameters, the frequency range and the damping ratio of the dampers. Three-dimensional plots were used to determine the optimum parameters that lead to the minimum RMS response. Table 7 gives

**TABLE 7. Optimum Damping Ratio and Frequency Range for MTLCD Configurations**

Cases (1)	Optimum damping ratio of each damper (%) (2)	Optimum frequency range (3)	RMS displacement (4)
No damper	—	—	12.53
$N = 1$ , STLCD	4.5	—	7.226
$N = 5$	1.4	0.12	6.927
$N = 11$	0.8	0.145	6.878
$N = 21$	0.6	0.155	6.864

Note: Values have been computed for white noise excitation,  $S_0 = 1$ ,  $\omega_s = 1$  rad/s,  $\zeta_s = 1\%$ ,  $\mu = 1\%$ .

**TABLE 8. Comparison of RMS Acceleration Responses of Each Floor due to Wind Loading**

Configuration (1)	Top level (cm/s <sup>2</sup> ) (2)	Fourth level (cm/s <sup>2</sup> ) (3)	Third level (cm/s <sup>2</sup> ) (4)	Second level (cm/s <sup>2</sup> ) (5)	First level (cm/s <sup>2</sup> ) (6)
Uncontrolled	5.81	5.21	4.48	3.57	2.36
1-STLCD	4.21	3.68	3.25	2.80	2.06
2-STLCD	4.25	3.76	3.30	2.74	1.99
1-MTLCD	4.19	3.66	3.24	2.80	2.06
2-MTLCD	3.98	3.52	3.10	2.61	1.93

the optimum parameters for different MTLCD groups. We note that the optimum damping ratio decreases drastically for MTLCD groups as compared to an STLCD.

#### Head-Loss Characteristics of MTLCDs

When tuning the orifices of each TLCD, the concept discussed in the previous section is applied to find the optimum head-loss coefficient for each tube to obtain similar orifice characteristic curves. It was noted that for a 5-TLCD group, the tuning characteristics of each liquid column orifice are almost similar. It is concluded that the damping characteristics of the TLCDs remain the same whether they are used in an STLCD or MTLCD configuration, although the optimal damping in both cases is different. This can be explained from (16) which relates the optimal damping to the RMS liquid velocity, cross-sectional area, and the head-loss coefficient. The cross-sectional area of each TLCD in MTLCD configuration is less than that for an STLCD. This is because the mass is distributed equally among all the TLCDs, so a portion of total liquid mass goes into each TLCD in the MTLCD configuration. This decrease in area corresponds to a decrease in optimal damping ratio (Table 7), while the head-loss coefficient remains the same in both systems.

#### Multiple Degrees of Freedom (MDOF)-MTLCD Configuration

Most of the previous work on multiple dampers has attempted to control only one mode (usually the first mode) of the primary system. However, this concept can easily be extended to multiple STLCDs and multiple MTLCDs placed strategically on various floors to reduce the higher modes as well. The time frequency analysis of several earthquake ground motion records utilizing wavelets has revealed the presence of higher frequency components in the initial stages of the event (e.g., El Centro) (Gurley and Kareem 1994). In such cases the presence of a second TLCD or MTLCD tuned to the second mode is essential in controlling motion induced by higher frequency components. The effectiveness of multiple dampers, spatially distributed in a structure was investigated

by Bergman et al. (1989). In the following, the effectiveness of structure-multiple-damper configurations is demonstrated with the aid of an example.

A 60-story building, 183 m in height, with a base area of  $31 \times 31$  m, was chosen and modeled as a 5-DOF system. The mass, stiffness, and damping matrices were taken from Li and Kareem (1990). The natural frequencies were determined to be 0.2, 0.58, 0.92, 1.18, and 1.34 Hz. After dynamic analysis, it was determined that the optimal location to place the dampers to effectively reduce the first and second mode was the top floor (fifth floor) and the second floor, respectively. Four configurations of dampers were studied and comparisons were made with an uncontrolled building. The multiple-mode configurations will be referred to as 2-STLCD and 2-MTLCD (2 refers to number of modes being controlled). In addition, the performance of 1-STLCD and 1-MTLCD also was examined. The response of the building under wind loads was estimated and the effectiveness of these damper configurations was studied. The spectral characteristics of wind loads are defined in Li and Kareem (1990).

In the preliminary design, equal mass ratios were assigned for the first and second modes (i.e., for 2-STLCD and 2-MTLCD) (0.5% each, total 1%). However, this caused adverse effects on the first mode response due to the presence of a second-mode TLCD, and the total response increased compared to 1-STLCD. This is because the presence of a TLCD tuned to the second mode decreases the effective damping in the first mode, which leads to an increase in the response. Similar observation has been made for multiple-TMDs by Rana and Soong (1998). To alleviate (if not completely eliminate) this problem, the placement of unequal mass ratios for different modes was considered. Peak response ratios were found to be in the ratio of 10:1 in the first and second modes. Therefore, mass ratios were distributed as 0.9 and 0.1% with a total of 1%. The performance of 1-STLCD and 2-STLCD is now comparable and 2-MTLCD provides an improvement in the performance. The optimum parameters were used in all the damper configurations. These were determined based on the theory presented in the previous sections. Table 8 shows a comparison of the RMS accelerations of the floors for a given wind loading for various configurations of dampers. From the table, one can note that 2-MTLCDs offer maximum reduction in response as compared to the other configurations. Additional advantages of multiple MTLCDs are given below:

- The robustness properties of MTLCDs are well known, so they are superior to STLCDs when there is an unexpected deviation from the optimal parameters. Moreover, the smaller value of optimal damping for MTLCDs makes them more attractive for liquid dampers, which have a limited range of damping ratios to work with as opposed to TMDs.
- The effectiveness of multiple MTLCDs for multimode response reduction has been shown. They clearly can be utilized effectively to suppress higher mode response in buildings.
- The MTLCDs offer smaller size than individual dampers (in terms of cross-sectional area and length). They can be installed in many possible locations. It is possible to save space by stacking MTLCDs inside each other.

#### CONCLUDING REMARKS

A method to determine the optimum damping in TLCDs, using a simplified solution to the integral occurring in the estimation of the mean square response, has been presented. The SDOF systems subjected to the white noise and FWN excitations have been analyzed, and the optimum absorber parameters for TLCDs have been determined. This work can be ex-

tended conveniently to MDOF systems utilizing a modal or state space approach.

Explicit expressions for optimal parameters are only feasible for a simple undamped primary system subject to white noise. As the systems and forcing functions become more complex, numerical solutions are needed to evaluate the optimal parameters. It has been noted that, for lightly damped systems, the optimal damping coefficient of the absorber does not depend on the damping coefficient of the primary system when the excitation is purely white noise. However, for the first- and second-order FWN cases, it is affected by the primary system damping. This suggests that the damping in the primary system plays a role in determining the optimum damping coefficient of the TLCD. Although the undamped case may yield an approximate value of the optimal absorber parameters, the primary system damping must be included for accurate estimates. This method is extended to determine the optimum head-loss coefficient, because it is apparent that the variance of the velocity of the liquid in the tube changes as the loading intensity changes. Therefore, to maintain the same level of damping, the head-loss coefficient needs to be adjusted by controlling the orifice opening ratio in the TLCD.

Optimal absorber parameters have been determined in the case of multiple TLCDs. These parameters include the number of TLCDs, the frequency range, and the damping ratio of each damper. It is noted that there is an upper limit on the number of TLCDs, beyond which additional TLCDs in the MTLCD configuration do not enhance the performance. The MTLCDs are more robust as compared to an STLCD, and the smaller value of the optimal damping makes them more attractive for liquid dampers that have a limited range of damping. The small size of individual TLCDs in an MTLCD configuration offers convenient portability and ease of installation at different locations.

## ACKNOWLEDGMENTS

The writers gratefully acknowledge the support provided by National Science Foundation, Washington, D.C., Grant CMS-95-03779 under the National Science Foundation Structural Control Initiative directed by Dr. S. C. Liu. The writers would like to thank Tracy Kijewski for her review of the manuscript.

## APPENDIX. REFERENCES

- Abé, M., Kimura, S., and Fujino, Y. (1996). "Control laws for semi-active tuned liquid column damper with variable orifice opening." *Proc., 2nd Int. Workshop on Struct. Control*, International Association for Structural Control, Hong Kong.
- Balendra, T., Wang, C. M., and Cheong, H. F. (1995). "Effectiveness of tuned liquid column dampers for vibration control of towers." *Engrg. Struct.*, 17(9), 668–675.
- Bergman, L. A., McFarland, D. M., Hall, J. K., Johnson, E. A., and Kareem, A. (1989). "Optimal distribution of tuned mass dampers in wind sensitive structures." *Proc., 5th Int. Conf. on Struct. Safety and Reliability*, ASCE, New York.
- Blevins, R. D. (1984). *Applied fluid dynamics handbook*, Van Nostrand Reinhold, New York.
- Clough, R. W., and Penzien, J. (1993). *Dynamics of structures*, 2nd Ed., McGraw-Hill, New York.
- Den Hartog, J. P. (1956). *Mechanical vibrations*, 4th Ed., McGraw-Hill, New York.
- Gao, H., Kwok, K. C. S., and Samali, B. (1987). "Optimization of tuned liquid column dampers." *Engrg. Struct.*, 19(6), 476–486.
- Grace, A. (1992). *MATLAB optimization toolbox user's guide*, Math-Works Inc., Natick.
- Gurley, K., and Kareem, A. (1994). "On the analysis and simulation of random processes utilizing higher order spectra and wavelet transforms." *Proc., 2nd Int. Conf. on Computational Stochastic Mech.*, Balkema, Amsterdam.
- Ioi, T., and Ikeda, K. (1978). "On the dynamic vibration damped absorber of the vibration system." *Bull. Japanese Soc. of Mech. Engrg.*, Tokyo, 21(151), 64–71.
- Kareem, A. (1981). "Wind-excited response of buildings in higher modes." *J. Struct. Div.*, ASCE, 107(4), 701–706.
- Kareem, A. (1983). "Mitigation of wind induced motion of tall buildings." *J. Wind Engrg. and Industrial Aerodynamics*, 11, 273–284.
- Kareem, A. (1984). "Model for predicting the across wind response of buildings." *Engrg. Structures*, 6, 136–141.
- Kareem, A. (1993). "Liquid tuned mass dampers: Past, present and future." *Proc., 7th U.S. Nat. Conf. on Wind Engrg.*, Wind Engineering Research Council, Vol. I.
- Kareem, A., and Kline, S. (1995). "Performance of multiple mass dampers under random loading." *J. Struct. Engrg.*, ASCE, 121(2), 348–361.
- Kijewski, T., Kareem, A., and Tamura, Y. (1998). "Overview of methods to mitigate the response of wind-sensitive structures." *Proc., Struct. Engrs. World Congr.*, Elsevier.
- Li, Y., and Kareem, A. (1990). "Recursive modeling of dynamic systems." *J. Engrg. Mech.*, ASCE, 116(3), 660–679.
- McNamara, R. J. (1977). "Tuned mass dampers for buildings." *J. Struct. Div.*, ASCE, 103(9), 1785–1798.
- Rana, R., and Soong, T. T. (1998). "Parametric study and simplified design of tuned mass dampers." *Engrg. Struct.*, 20(3), 193–204.
- Randall, S. E., Halsted, D. M., and Taylor, D. L. (1981). "Optimum vibration absorbers for linear damped systems." *J. Mech. Des.*, 103, 908–913.
- Roberts, J. B., and Spanos, P. D. (1990). *Random vibration and statistical linearization*, Wiley, New York.
- Sakai, F., and Takaeda, S. (1989). "Tuned liquid column damper—New type device for suppression of building vibrations." *Proc., Int. Conf. on High Rise Build.*, Nanjing, China, 926–931.
- Soong, T. T., and Dargush, G. F. (1997). *Passive energy dissipation systems in structural engineering*, Wiley, New York.
- Warburton, G. B. (1982). "Optimal absorber parameters for various combination of response and excitation parameters." *Earthquake Engrg. and Struct. Dyn.*, 10, 381–401.
- Warburton, G. B., and Ayorinde, E. O. (1980). "Optimum absorber parameters for simple systems." *Earthquake Engrg. and Struct. Dyn.*, 8, 197–217.
- Xu, Y. L., Samali, B., and Kwok, K. C. S. (1992). "Control of along-wind response of structures by mass and liquid dampers." *J. Engrg. Mech.*, ASCE, 118(1), 20–39.
- Yalla, S. K., and Kareem, A. (1998). "Optimal parameters for TLCDs." *Tech. Rep. No. NDCE 98-002*, Dept. of Civ. Engrg. and Geological Sci., University of Notre Dame, Notre Dame, Ind.
- Yalla, S. K., Kareem, A., and Kantor, J. C. (1998). "Semi-active control strategies for tuned liquid column dampers to reduce wind and seismic response of structures." *Proc., 2nd World Conf. on Struct. Control*.